Chapter 18
NOESY

Michael P. Williamson

Department of Molecular Biology and Biotechnology, University of Sheffield, Firth Court, Western Bank, Sheffield S10 2TN, UK

18.1 INTRODUCTION

The Nuclear Overhauser Effect (NOE) is a relaxation phenomenon that is used very widely in solution-state NMR because it gives direct and readily interpretable information on short internuclear distances, which can then be used to derive structural details. It is closely related to dipolar coupling. A wide variety of experiments have been developed to measure NOEs. One of the most commonly used experiments is the 2D NOE experiment, generally known by the acronym NOESY (2D Nuclear Overhauser Effect SpectroscopY), introduced by the inventors of the experiment, Macura and Ernst.[1] The NOESY experiment (including the various 3D and 4D heteronuclear versions, which are essentially 2D NOESY spectra with a heteronuclear transfer tacked on) is most commonly applied to the assignment and structure determination of biological macromolecules, whereas for small organic molecules, 1D experiments remain very common, as discussed below.

NOESY experiments are simple to set up, and simple to interpret in a qualitative way, namely that a NOESY cross peak connecting two signals implies a short distance between them. The spectra are normally presented as square plots containing a line of diagonal peaks and symmetrically placed cross peaks (Figure 18.1). The 3D heteronuclear analogs are identical, except that one does not normally show the whole plane, and the spectra are no longer symmetrical.[2] The spectra are normally presented as contour plots for ease of analysis. Although they are in principle symmetrical about the diagonal, in practice they are not completely symmetrical because of different digital resolution and processing parameters in the two dimensions, relaxation effects, and experimental artifacts. The two dimensions are distinguished by the labels F_1, F_2 (or sometimes Ω_1, Ω_2; ω_1, ω_2; ν_1, ν_2; or even the incorrect t_1, t_2), where 1 and 2 refer, respectively, to the indirectly and directly detected dimensions (see below). There is no convention as to which dimension is drawn as the y axis, but more normally the F_1 axis would be vertical.

Cross peaks with nonzero net intensity originate from *cross relaxation* between the two nuclei at the frequencies of the cross peak: that is, from relaxation processes where both nuclear spins flip simultaneously (see 18.2). Cross relaxation only occurs between nuclei that are close together, and hence a cross peak is readily interpreted as a close distance

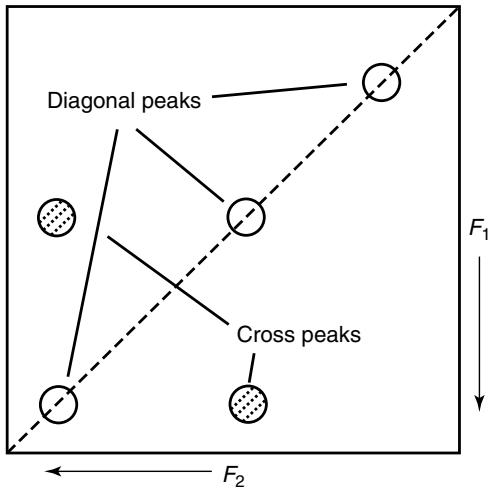

Figure 18.1. The basic elements of a NOESY spectrum.

between the two nuclei at the chemical shifts of the cross peak. The meaning of "close" obviously depends upon the molecule under investigation and the sensitivity of the experiment, but it may generally be taken to mean within about 5 Å, except in cases of severe spin diffusion where a longer distance is possible. The relationship between distance and cross-peak intensity is discussed below and is not straightforward, but in many cases a very crude measure of intensity is sufficient to provide the required structural information.

NOESY is a method of measuring magnetization transfer between pairs of nuclei. It is therefore equally as good at measuring chemical exchange as it is at measuring NOEs, and the same experiment is used for both measurements (see Chapter 21).

18.2 THE NOE

Only a very brief account is presented here, limited to $^1H-^1H$ NOEs. The NOE is covered in more detail in the Encyclopedia of Magnetic Resonance and also in a book and review.[3,4]

If the longitudinal (z) populations of a nucleus are perturbed, for example, if the populations are equalized by saturation, then the nucleus will relax back toward equilibrium. It will normally do this by T_1 relaxation: spins flip, and the energy released (or required) by the flip is given to (or taken from) the surrounding atoms ("the lattice") in the form of heat. It is important to note that *spontaneous* relaxation is extremely slow: the spin flip needs to be stimulated, most commonly by fluctuations in the local magnetic field at the nucleus, caused by motion of the molecule. The fluctuations need to be occurring at a rate similar to the energy difference corresponding to the spin flip. For example, for protons in a 500 MHz spectrometer, the molecular motion should have a component at a frequency of 500 MHz in order to stimulate spin–lattice relaxation.

If there are two nuclei close together, an alternative relaxation process is possible: *both* spins can flip simultaneously. This can happen in two different ways: (i) both spins can flip together in the same direction, or (ii) a "flip-flop" process can occur where one spin goes from up to down and the other from down to up. Both of these processes lead to relaxation of the perturbed spin toward equilibrium, but in the process they perturb the populations of the neighbor. If the perturbed spin has been saturated, then pathway (i) leads to an increase in the population difference of its neighbor, while pathway (ii) leads to a reduction in the population difference. Thus, relaxation leads to an increase in the intensity of the signal from the neighbor in case (i) and a reduction in case (ii). These are called a *positive* and a *negative NOE*, respectively. The two pathways again need to be stimulated by molecular motions at the appropriate frequency, which, for (i), is twice the single-spin frequency, or 1000 MHz, and, for (ii), is the difference in frequency between the two proton transitions, i.e., their chemical shift difference, which is of the order of kilohertz. Therefore, the probability of pathways (i) and (ii), or, in other words, whether a positive or negative NOE results, depends on the tumbling rate of the molecule: for small molecules with high-frequency motions the NOE is positive, while for large molecules the NOE is negative (Figure 18.2). Obviously at some point in the middle, the NOE is zero.

18.3 THE NOESY EXPERIMENT: THEORY

18.3.1 The Pulse Sequence

The NOESY pulse sequence is shown in Figure 18.3, and consists simply of three pulses, each of 90°. The simplest system required to understand the pulse sequence is a system of two protons I and S that are

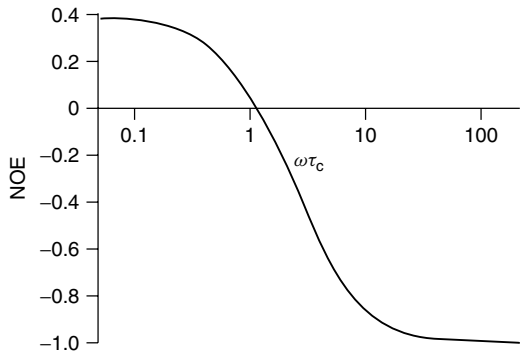

Figure 18.2. The dependence of the maximum possible NOESY effect on molecular tumbling rate, given as the product of the Larmor angular frequency (= $2\pi \times$ spectrometer frequency) and the correlation time (the time for a significant change in molecular orientation). The zero crossing point corresponds roughly to medium-sized peptides in water: proteins are well over to the right, while most organic molecules in organic solvents are well to the left.

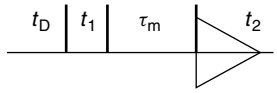

Figure 18.3. The NOESY pulse sequence. The vertical bars represent 90° pulses.

not spin–spin coupled. The first pulse converts longitudinal z magnetization into transverse magnetization (Figure 18.4). In product operator nomenclature,[5,6] this corresponds for spin I to $I_z \rightarrow -I_y$. During the subsequent period t_1, the magnetization precesses around the z axis, so that at the end of t_1 each nucleus has precessed through an angle ωt_1, where ω is the angular frequency of the nucleus compared with the reference frequency, or in other words its chemical shift difference from the carrier: $-I_y \rightarrow (-I_y \cos \omega_I t_1 + I_x \sin \omega_I t_1)$. The second pulse rotates this magnetization around the pulse axis, so that an x pulse produces magnetization in the xz plane: $(-I_z \cos \omega_I t_1 + I_x \sin \omega_I t_1)$. The phases of the pulses are cycled in subsequent pulse sequences so that any transverse magnetization following the second pulse is canceled out, leaving only the component $-I_z \cos \omega_I t_1$. The first two pulses have therefore achieved a *frequency labeling* of magnetization, in which each magnetization vector now has only a longitudinal intensity, modulated both by t_1 and by its chemical shift.

The period between the second and third pulses is the mixing period τ_m during which the NOE develops by cross relaxation. At the start of τ_m, the two spins in general have nonequilibrium magnetization, $-I_z \cos \omega_I t_1$ and $-S_z \cos \omega_S t_1$, respectively. They therefore cross-relax each other as described in 18.2, as a result of which their magnetization at the end of τ_m is different: each has acquired some fraction of the magnetization of the other, giving an intensity $(-a_I I_z \cos \omega_I t_1 + a_{IS} S_z \cos \omega_S t_1)$ for nucleus I and $(-a_S S_z \cos \omega_S t_1 + a_{IS} I_z \cos \omega_I t_1)$ for nucleus S. The z magnetization is read by the final pulse, which converts it to transverse magnetization. During t_2, the I and S transverse magnetizations precess at the frequencies of I and S respectively, meaning that in each case the first term gives rise to the diagonal peak, and the second term gives rise to the cross peak. Finally, the relaxation delay t_D allows magnetization to relax back toward equilibrium before the start of the next pulse sequence. As in all 2D experiments, the experiment is repeated for a series of regularly incremented t_1 values and stored as a matrix of points in t_1 and t_2: Fourier transformation with respect to t_1 and t_2 results in frequencies in both dimensions in the normal way.

18.3.2 NOE Buildup During τ_m: Initial Rate

A nucleus I in the presence of other nuclei S will relax at a rate:[3]

$$dI_z/dt = -R_I \left(I_z - I_z^0\right) - \sum_S \left(S_z - S_z^0\right) \sigma_{IS} \tag{18.1}$$

where R_I is the longitudinal relaxation rate for spin I (roughly the inverse of T_1), I_z^0 is the equilibrium value of I_z, $S_z^0$is the equilibrium value of S_z, and σ_{IS} is the cross-relaxation rate between I and S, which is given by

$$\sigma_{IS} = \frac{K^2}{10}\left[\frac{6\tau_c}{1+(\omega_I+\omega_S)^2\tau_c{}^2} - \frac{\tau_c}{1+(\omega_I-\omega_S)^2\tau_c{}^2}\right] \tag{18.2}$$

where

$$K = (\mu_0/4\pi)\hbar\, \gamma_I\, \gamma_S\, r_{IS}^{-3} \tag{18.3}$$

In equations (18.2) and (18.3), ω_I and ω_S are the Larmor frequencies for nuclei I and S, respectively, in radians per second, which are a factor of 2π greater

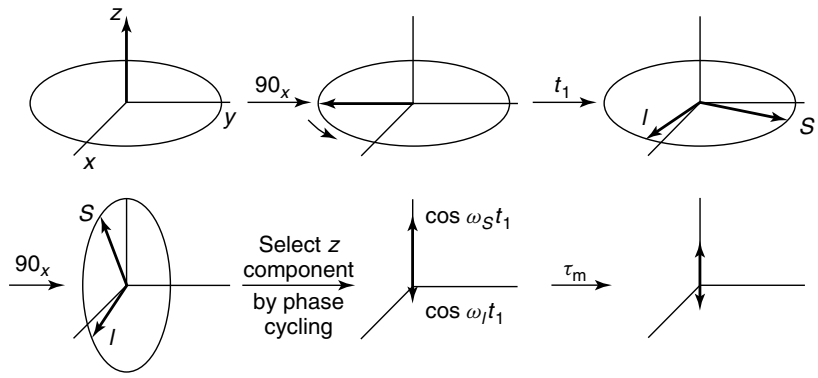

Figure 18.4. Magnetization of two spins I and S in a NOESY pulse sequence.

than the spectrometer frequencies in hertz, and τ_c is the correlation time of the molecule, which is a measure of the time it takes to reorient. γ_I and γ_S are the gyromagnetic ratios of the two nuclei, and r_{IS} is the distance between I and S. The equations are only valid for an isotropically tumbling rigid molecule, and throughout we assume a homonuclear NOE, in particular, between two protons.

These equations express what was described in 18.2 and 18.3.1. They mean that if S_z is not at its equilibrium value, it will cause the intensity of I_z to change at a rate proportional to $r_{IS}{}^{-6}$. Likewise, if I_z is not at its equilibrium value, it will cause the intensity of S_z to change in the same way. They form a set of coupled differential equations, which can be solved using matrix algebra,[3] with the simple result that at short τ_m, cross-peak intensities a_{IS} are directly proportional to $\sigma_{IS}\ \tau_m$. This result explains why the NOE, and NOESY in particular, is so widely used for structural studies: *at short mixing times, the intensity of cross peaks in NOESY is proportional to* $r_{IS}{}^{-6}$. Thus, for example, given a suitable known calibration distance r_{ref}, one measures the intensity of the corresponding cross peak a_{ref}, and uses this to measure other distances using the simple formula

$$r_{IS} = r_{ref}\left[\frac{a_{IS}}{a_{ref}}\right]^{-1/6} \qquad (18.4)$$

This equation is the basis of all NOE-based structure calculations. However, for all practical applications, there are a number of major qualifications that need to be made, which mean that one has to be much less precise than would be implied by equation (18.4). These are considered in the following section.

18.3.3 NOE Buildup During τ_m: Real Life

Most of the details that we need to consider arise when considering a simple three-spin molecule, with nuclei A, B, and C in a straight line. NOESY intensities for such a molecule are shown in Figure 18.5, for large and small molecules in (a) and (b), respectively.

1. All enhancements rise rapidly and decay more slowly. The initial rise is at a rate σ_{IS}, as described above, and the decay is approximately the T_1 decay rate. The maximum enhancement is reached for different cross peaks at different times.
2. There is an "initial rate region" at short τ_m, in which each pair of protons can be treated as an isolated spin pair, and thus NOESY intensities follow equation (18.4). However, this region is short and its duration is strongly dependent upon the geometry of the spins: in the example shown in Figure 18.5, the initial rate region is longer for the strong direct enhancement A–B than for the A–C enhancement, for which the indirect enhancement A–B–C rapidly dominates. Moreover, it is much longer in Figure 18.5(b) than in Figure 18.5(a), in which it lasts no more than 5 ms (see inset in Figure 18.5a). It is usually not possible to measure intensities accurately at very short mixing times because they are too small: therefore, in practice, one cannot be confident that NOE intensities truly follow equation (18.4).

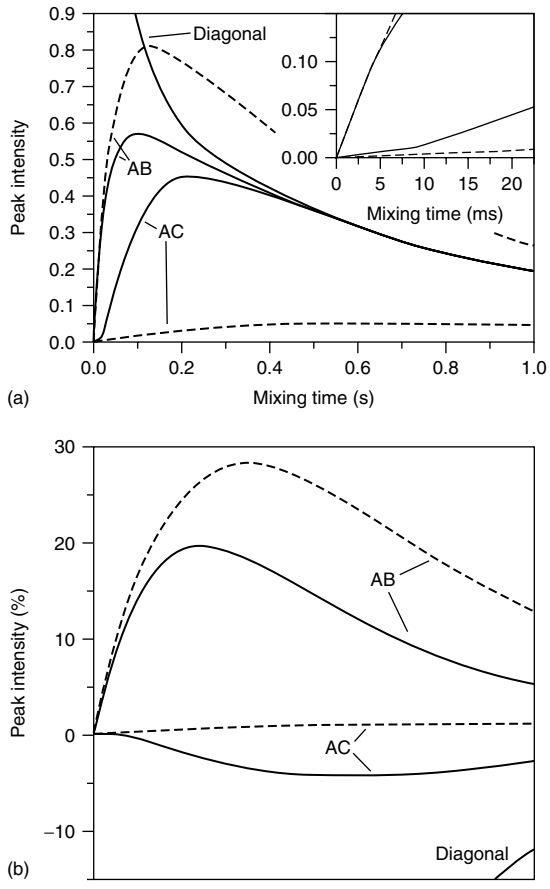

Figure 18.5. The dependence of cross-peak and diagonal peak intensity on τ_m in a NOESY experiment. The curves are for a three-spin system with nuclei A, B, and C, which are in a straight line with $r_{AB} = r_{BC} = 2.5$ Å, and show the intensities of the A diagonal peak and the AB and AC cross peaks. The correlation time τ_c is 5×10^{-8} s in (a), as appropriate for a biological macromolecule, and 10^{-10} s in (b), as appropriate for an organic molecule in a nonviscous solvent, and the spectrometer frequency is 500 MHz (i.e., $\omega_0 = 2\pi \times 5 \times 10^8$, $\omega_0\tau_c = 157$ and 0.3 for (a) and (b), respectively). The inset in (a) shows an expansion of the initial part of the curve. External relaxation at a rate 10% of the dipolar cross-relaxation rate is included. The curves marked by dashed lines are the equivalent curves for the two-spin systems A–B and A–C; these are the curves of the "isolated spin pair approximation". The diagonals have initial intensities of 2.0 and −200 in (a) and (b), respectively. Note that the absolute phases are arbitrary, and the direct AB cross peak has been presented as a positive signal in (b) merely because this is the normal presentation. Calculated using a numerical method.[8]

3. For large molecules such as proteins (Figure 18.5a), the NOE goes from *A* to *B*, but then is passed on rapidly from *B* to *C*, so that the NOE observed at *C* is much larger than would be expected from the direct *A*–*C* distance. This process is known as *spin diffusion*, and is the main reason that NOESY cross-peak intensities cannot be used simply as implied by equation (18.4): see, for example, the very large difference in NOE intensity between the solid and dashed lines for the *AC* NOE in Figure 18.5. In theory, by observing the cross-peak intensity at very short τ_m it should be possible to distinguish the two cases, because the indirect NOE has a lag period before it starts to build up (Figure 18.5a, inset). However, in practice, the signal-to-noise ratio at short τ_m is low and such observations are difficult. Therefore, in practice, one uses a τ_m that produces measurable but noninitial NOE intensities (such as 50–100 ms), and then uses a calibration that is much looser than equation 18.4. A common, though unnecessarily arbitrary and imprecise, method is to define NOEs as strong, medium, and weak, corresponding, for example, to distances of <2.5 Å, <3.5 Å, and <5 Å, respectively: alternatively, one can just set the upper distances longer than those given by equation (18.4).
4. For protons that are very close together, cross-peak intensities rise rapidly and also decay rapidly. This implies that the reference distance r_{ref} should be comparable to the distance being measured; in particular, it is bad practice to use the NOE between a pair of methylene (CH_2) protons as a reference, because the resultant calibration will be inaccurate.
5. During the later stages of cross-peak evolution, spin diffusion ensures that cross-peak intensities in macromolecules become increasingly similar (Figure 18.5a). Hence, the distance information that can be obtained from cross-peak intensities diminishes as τ_m increases, although the intensities of weak cross peaks tend to be greater. Therefore, it is fairly common to use two NOESY experiments with different τ_m: a long value to observe weak NOEs, and a shorter one to get more accurate distances.
6. The sign of the direct cross peaks relative to the diagonal peaks is opposite for large molecules (Figure 18.5a) and for small

molecules (Figure 18.5b). The sign changes when $\omega_0\tau_c = (5/4)^{1/2} = 1.12$.[3] The molecular size corresponding to the crossover point is hard to define as τ_c can vary strongly with solvent viscosity and solute interactions, but it tends to be at the oligopeptide stage in water or rather larger in less viscous organic solvents. One implication of this is that NOEs in peptides can be small and unpredictable. For such cases, it is preferable to use a different experiment called *ROESY*,[7] in which a spin-locking field is applied during τ_m (see Chapter 19). This makes all molecules behave as though they were small molecules, and therefore peak intensities in ROESY are as in Figure 18.5(b) (see below).

7. For small molecules (Figure 18.5b), the indirect or spin-diffusion NOE from *A* to *C* has the opposite sign from the direct *AB* NOE, and is also much smaller. It is therefore usually easy to distinguish such "three-spin effects" from direct NOEs in small molecules.
8. Peaks in NOESY or ROESY arising from chemical exchange are always in phase with the diagonal. Therefore for small molecules and in ROESY spectra, exchange is easy to identify. For macromolecules, the two effects are usually obviously distinguishable, from the chemistry of the molecule or from the different rates of the two processes, but in ambiguous cases a distinction can usually be made by raising the temperature, where in general cross relaxation gets slower but exchange gets faster.
9. Equation (18.4) only applies to rigid molecules. In practice, most macromolecules have some more mobile regions, and in these regions NOEs are smaller or even nonexistent. One implication of this is that while observation of an NOE is evidence for proximity (subject to spin diffusion), *absence* of an NOE must be interpreted with great caution. Further, if a molecule is in equilibrium between two conformations, then the observed NOE is an r^{-6} average: this implies that small populations of different conformations can give rise to relatively large NOEs (and therefore very misleading information) if there is a short internuclear distance present. Equation 18.4 is also only valid for molecules that tumble with the same rate in all directions (isotropically). For very asymmetric molecules, the cross-relaxation rate depends also on orientation.

18.4 THE NOESY EXPERIMENT: PRACTICE

18.4.1 The Setting of Experimental Parameters

Most experimental parameters for NOESY are very easy to set. All pulse widths should be 90°. Ideally, the delay t_D should be long enough that all signals have relaxed back to equilibrium by the end of t_D, implying 3–5 times the longest T_1. In practice one cannot wait that long. A value that is too short leads to NOEs that are too small for slowly relaxing nuclei, and to cross-peak intensities that are different on opposite sides of the diagonal. In practice, a value of 0.7 s is often adequate for macromolecules, unless they are very large or if very high fields are used, where T_1 relaxation is slower. For small molecules, longer delays are necessary.

The most critical parameter is the delay τ_m. To obtain optimum sensitivity, a value should be chosen such that cross peaks are at their maximum intensity. This time will be different for each pair of protons, and it varies strongly with the correlation time of the molecule. It is of the same order as the T_1 relaxation time, and for a small globular monomeric protein in water is roughly 250 ms. For a large protein or long DNA molecule, it can be 20 ms or less, while for small molecules in organic solvents it can be well over 1 s (as in Figure 18.5b).

However, the main concern in NOESY experiments is usually not sensitivity but structural information. The points outlined in 18.3.3 imply that any direct relationship between cross-peak intensity and internuclear distance is only obtained for short τ_m values, and even here it is not normally feasible to relate cross-peak intensity directly to distance.

Two approaches have been taken to this problem. The first is to choose τ_m values as short as possible, and use an empirical calibration to relate intensity to distance.[9] Thus, the sequential distance HN–HN in a protein α-helix is normally about 2.8 Å. If sequential HN–HN NOESY cross peaks in helical regions are found to have intensities (in arbitrary units) ranging from 100 to 300, then one can make the conservative estimate that cross peaks with intensities of 100 or greater correspond to a distance of 2.9 Å or less. Further empirical calibrations are made using other predictable internuclear distances.

The second approach uses the exact solution of the relaxation matrix equation. The difficulty with this approach is that one can only apply the equation if all internuclear distances are known, and it is exactly this information that one is trying to derive. The typical approach is therefore to iterate toward a solution.[10] Using the isolated spin pair approximation, initial values are obtained for cross-relaxation rates and hence internuclear distances. These values are used to produce a structure from which relaxation rates are calculated. These derived rates are combined with experimentally determined rates to produce a hybrid relaxation matrix, and the process is iterated until it converges, which typically occurs after only one or two iterations. In most cases, such an approach is not necessary: the most common application is to DNA structures, where spin diffusion is particularly troublesome, and accurate distance calibrations are particularly important.

The number of points in t_2 is limited only by disk space and the required resolution, and is typically 2 k or 4 k complex points. With larger molecules, the signal may well have decayed to zero long before this, in which case fewer points are necessary. By contrast, it is not generally feasible to collect so many points in t_1, and the maximum value of t_1 (i.e., the number of increments) is always a compromise between sensitivity and time pressure (which require fewer points) and resolution (which requires more points). Typically, 300–512 complex points are acquired. If too few t_1 points are acquired, the interferogram will be severely truncated (i.e., it will be cut off before it has decayed to zero). Fourier transformation of truncated FIDs produces "sinc wiggles" around each peak (Figure 18.6a), which can be reduced but not eliminated by a suitable window function. Such wiggles are particularly evident in 2D spectra around the diagonal peaks of sharp intense resonances such as methyl groups, which have signals that decay slowly in t_1 (Figure 18.6b).

The increments in both dimensions depend on the spectral widths. In t_1, there is no point in acquiring over a spectral width wider than that defined by the signals of the sample. Greater resolution is obtained by using a spectral width smaller than the entire range, but unless selective pulses are used, this strategy runs the risk of severe complications from the folding in of signals from outside the spectral width, since no filter is applied to such signals.

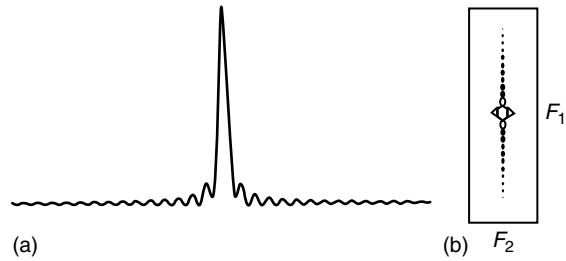

Figure 18.6. The effect of truncation is to give sinc wiggles. (a) Sinc wiggles in 1D. (b) Sinc wiggles in the F_1 dimension resulting from truncation in t_1.

18.4.2 Experimental Artifacts

An artifact is an unwanted signal. It may arise from a defect in the spectrometer or be inherent in the physics of the experiment, but it can be minimized by appropriate experimental design. Most of the artifacts arising from spectrometer defects are now insignificant due to greatly improved spectrometer design. These include t_1 noise (bands of noise parallel to the F_1 axis), temperature artifacts (usually visible as ridges parallel to the diagonal), shimming problems (cross peaks elongated parallel to the diagonal) and quadrature images (diagonal and cross peaks reflected around the center of the spectrum). Many of the remaining artifacts are removed by the *phase cycle* that is part of the pulse sequence. In a phase cycle, one acquires a signal using some set of phases for the pulses and receiver. Then one uses a different set of phases and adds the two signals together. With correctly chosen phases, the desired signal will add coherently, while unwanted signals will be canceled out. Phase cycles are thus normally built up from pairs of experiments, and so are typically 2^n long. Table 18.1 lists a typical NOESY phase cycle.

Between steps 1 and 2, the phases of the first and third 90° pulse are inverted, and the two experiments are added together. From Figure 18.4 (and/or from the product operators: a very instructive exercise but rather tedious), it is clear that the resultant signal is identical. However, unwanted signals arising from magnetization that is transverse during τ_m (i.e., the I_x and S_x components), and from longitudinal relaxation during τ_m (which gives rise to "axial peaks" that come at zero frequency in F_1) are canceled out. Coaddition of steps 3 and 4, 5, and 6 has the same effect; thus, at every other step these unwanted signals are removed.

Table 18.1. Phase cycle for the suppression of artifacts in NOESY

Step	90°	90°	90°	Acquisition
1	x	x	x	x
2	$-x$	x	$-x$	x
3	y	y	x	x
4	$-y$	y	$-x$	x
5	x	x	y	y
6	$-x$	x	$-y$	y
7	y	y	y	y
8	$-y$	y	$-y$	y
9	x	x	$-x$	$-x$
10	$-x$	x	x	$-x$
11	y	y	$-x$	$-x$
12	$-y$	y	x	$-x$
13	x	x	$-y$	$-y$
14	$-x$	x	y	$-y$
15	y	y	$-y$	$-y$
16	$-y$	y	y	$-y$

Steps 1–3, 2–4, etc., remove artifacts arising from J-coupling between the two spins. The NOESY pulse sequence has three 90° pulses and thus has the same form as the double-quantum filtered COSY (DQ-COSY) pulse sequence, which gives cross peaks for J-coupled spins. The only differences between them are the length of τ_m (which is very short for DQ-COSY) and the phases: in DQ-COSY, phases are chosen specifically to keep J-coupled signals while in NOESY they are chosen to remove them. This phase cycle is discussed in more detail in 18.4.2.1.

Finally, it will be seen that in steps 1, 5, 9, and 13 (and of course in 2, 6, 10, and 14), the third pulse and receiver are cycled around the phases x, y, $-x$, $-y$. This cycle is known as *CYCLOPS* and removes quadrature artifacts. These are the least serious artifacts and CYCLOPS is therefore done as the slowest cycle.

The most obvious implication of the discussion above is that an incomplete phase cycle will leave artifacts: one should therefore always try to use a number of scans that is a multiple of the phase cycle. However, because the most essential elements of this phase cycle are contained in the first group of four steps, use of a phase cycle that is a multiple of 4 rather than 16 steps will only lead to increased quadrature images, and will not hinder the workings of the rest of the phase cycle.

Biological molecules are usually observed in H_2O, implying that there will be residual signal from the solvent, evident as a stripe of noise at the frequency of water parallel to the F_1 axis. This can be minimized very successfully by appropriate data processing. If the receiver gain of the spectrometer is turned up too high so that incoming solvent signal is clipped in the spectrometer memory, the spectrum becomes impossibly noisy. The only solution is to rerun the experiment with lower receiver gain.

18.4.2.1 J Peaks

So far we have almost ignored much of the magnetization created by the NOESY pulse sequence. This can be calculated using the product operator formalism as follows.

For the pulse sequence 90°_x, t_1, 90°_x, τ_m, 90°_x, acquire, operating on a system containing two protons I and S, dipolar coupled and spin–spin coupled with a coupling constant J, the first pulse has the effect $I_z \rightarrow -I_y$, and similarly on S:$S_z \rightarrow -S_y$. During t_1, the spins evolve under the influence of chemical shift and J-coupling to give equation (18.5):

$$\begin{aligned} -I_y \longrightarrow\ & (-I_y \cos\omega_I t_1 + I_x \sin\omega_I t_1)\cos\pi J t_1 \\ & + (2I_x S_z \cos\omega_I t_1 + 2I_y S_z \sin\omega_I t_1)\sin\pi J t_1 \\ -S_y \longrightarrow\ & (-S_y \cos\omega_S t_1 + S_x \sin\omega_S t_1)\cos\pi J t_1 \\ & + (2S_x I_z \cos\omega_S t_1 + 2S_y I_z \sin\omega_S t_1)\sin\pi J t_1 \end{aligned} \tag{18.5}$$

The second 90° pulse rotates all these components about the x axis, giving a total magnetization as in equation (18.6):

$$\begin{aligned} & (-I_z \cos\omega_I t_1 + I_x \sin\omega_I t_1)\cos\pi J t_1 \\ + & (-2I_x S_y \cos\omega_I t_1 - 2I_z S_y \sin\omega_I t_1)\sin\pi J t_1 \\ + & (-S_z \cos\omega_S t_1 + S_x \sin\omega_S t_1)\cos\pi J t_1 \\ + & (-2S_x I_y \cos\omega_S t_1 - 2S_z I_y \sin\omega_S t_1)\sin\pi J t_1 \end{aligned} \tag{18.6}$$

The only components required for the NOE observation are those in S_z and I_z; these are the components that exchange magnetization by cross relaxation during τ_m and are observed as single-quantum magnetization after the final pulse. All the other components give rise to various undesirable signals in the NOESY spectrum and should be removed.

The single-quantum in-phase and antiphase components, $I_x \sin\omega_I t_1 \cos\pi J t_1 - 2I_z S_y \sin\omega_I t_1 \sin\pi J t_1 + S_x \sin\omega_S t_1 \cos\pi J t_1 - 2S_z I_y \sin\omega_S t_1 \sin\pi J t_1$, continue to evolve during τ_m and are converted by the final pulse to various in-phase and antiphase signals (including in-phase cross peaks) as well as other unobservable components. The former would produce

diagonal and cross peaks in the same positions as found in COSY and relayed COSY spectra. They are easily removed by phase cycling, as described above. For example, the pulse sequence 90°_{-x}, t_1, 90°_{-x}, τ_m, 90°_x, which we write in shorthand as $(-x, -x, x)$, can be easily shown to produce the same z magnetization during τ_m but inverted single-quantum magnetization. Thus, coaddition of the results from these two pulse sequences will remove all signals resulting from magnetization that was single quantum during τ_m.

The other unwanted contributions are the terms $-2I_xS_y\cos\omega_I t_1 \sin \pi J t_1 - 2S_xI_y\cos\omega_S t_1 \sin \pi J t_1$, which describe a mixture of double- and zero-quantum coherence, and are partially converted back to antiphase single-quantum coherence by the third pulse. They both survive the phase cycle described above. The double-quantum coherence can be removed by the phase cycle $(x, x, x) + (y, y, x)$: this is readily understood by comparison with the previous phase cycle, because double-quantum coherence is twice as sensitive to pulse phase changes as is single-quantum magnetization, and therefore only requires a 90° phase change of the first two pulses.[11]

The zero-quantum coherence cannot be removed by a phase cycle, because it is affected by phase cycling in an identical manner to the desired z magnetization. It can, however, be removed by making use of the fact that zero-quantum magnetization precesses during τ_m. Therefore, coaddition of several suitably chosen experiments with slightly different τ_m will lead to (partial) cancellation of such terms, while those arising from z magnetization will be unaffected except that slightly different amounts of cross relaxation will have occurred. On many spectrometers, this is accomplished by a random variation of τ_m by about 20 ms. Note that the random variation should only occur between iterations of a phase cycle and not during it; if τ_m is altered during a phase cycle, the zero-quantum contribution and the other J peaks are smeared out in F_1 rather than being neatly removed.

One final type of J peak can arise if the pulses are not 90°. In this case, magnetization of the type I_zS_z can be produced and partially converted back to single-quantum antiphase magnetization by the final pulse. This again produces COSY-type antiphase peaks for J-coupled protons, which are most simply avoided by calibrating the pulse length carefully or if necessary using a composite pulse.[11] Relaxation of I_zS_z magnetization, also known as *longitudinal two-spin order*, is of interest in its own right, but the NOESY experiment is not an efficient experiment for its study. Rather, experiments using low flip angles or selective pulses are preferable.

18.4.3 Data Processing

In NOESY, data processing is simple and consists largely of finding the best filters for the data, phasing the spectrum, and flattening the baseplane. The data are not greatly sensitive to the filters used and phase-shifted sine-bell or sine-squared-bell filters are often suitable. Phasing is independent in the two dimensions.[12] Normally, phasing in t_2 can be determined by phasing the first FID of the 2D file, while the appropriate phase in t_1 can be worked out from the initial delay between the first two pulses, and is almost always zero or 90°.

18.5 APPLICATIONS OF NOESY

18.5.1 When Should NOESY be Used?

The NOE is the most widely used structural parameter in organic and biological NMR. The main experiments used for measuring NOEs are NOESY, ROESY, and 1D experiments such as NOE difference and the gradient-selected experiment.[13] The choice of which experiment to use is essentially dictated by the size and correlation time of the molecule.

In small molecules, cross relaxation is slow. NOEs therefore build up slowly and external relaxation competes favorably with the NOE. NOESY is therefore often very insensitive and takes a long time because of the long relaxation delays required (Figure 18.5b). By comparison, 1D methods are usually more sensitive. In addition, in small molecules, there is usually no difficulty in achieving the specific irradiation required because there are fewer signals present. It is therefore generally preferable to use 1D methods, of which the gradient-selected experiment is gradually replacing "classical" 1D NOE difference, despite its lower sensitivity, because of its lack of artifacts. However, in cases where there are many irradiation targets, it can be more time-efficient to use NOESY or ROESY experiments (see Chapter 19).

As the size of the molecule under investigation increases, and therefore the correlation time τ_c of the molecule increases, the maximum homonuclear NOE goes through zero (Figure 18.2), and both

the 1D NOE and the NOESY experiments become insensitive. However, cross relaxation in the rotating frame is still very significant and so ROEs can still be observed. This is therefore the only experiment useful in the region around $\omega_0\tau_c = 1.12$.

Above this point, NOESY is usually more sensitive, easier to set up, and produces fewer artifacts, and is therefore generally preferred over ROESY or 1D methods. However, the problem of spin diffusion is less severe in ROESY than in NOESY. This is because in ROESY, as in all cases where $\omega_0\tau_c < 1.12$, a relayed or spin diffusion NOE has the opposite sign to a direct NOE and therefore can be easily distinguished. There are therefore good reasons for using ROESY even for very large molecules. Further discussion of these points may be found elsewhere.[3]

18.5.2 Studies of Macromolecules

NOESY is the most widely used technique for measuring NOEs in large molecules such as proteins and nucleic acids. Many examples may be found elsewhere (see Chapters 33 and 34). NOESY is an excellent tool for obtaining qualitative information about internuclear distance, but not as good at providing quantitative information. In part, this is because the most reliable quantitative information is obtained at very short mixing times where the sensitivity is lowest and artifacts are most prominent, and also because it is not easy to integrate the volume of NOESY cross peaks accurately, particularly in crowded spectra. NOEs can only be interpreted quantitatively when the dynamics of the system are well characterized, and in almost all cases not enough is known about the internal dynamics of macromolecules in solution to allow the full precision of the data to be used. Nevertheless, many studies have shown that loose restraints can still produce high-quality structures, as long as there are enough of them.

For macromolecules, spectral crowding is a major problem. Therefore, the large majority of NOESY spectra of proteins use isotopically labeled protein, and 3D or even 4D spectra, where the extra dimensions are heteronuclear frequencies (see Chapter 25). A popular 3D NOESY experiment acquires NOEs for ^{15}N- and ^{13}C-coupled protons simultaneously;[14] dimensions 1 and 2 are the indirect ^{1}H and ^{15}N/^{13}C ^{1}J-coupled frequencies, and the direct third dimension is protons receiving NOEs from the indirectly detected protons. This gives much improved resolution and has had a major impact on the ease of assignment of NOEs to specific protons. Sensitivity losses from the heteronuclear transfer are small for fully labeled proteins, and therefore the experiments have excellent signal-to-noise ratio. Just as a 2D spectrum requires a series of t_1-incremented 1D FIDs, so a 3D spectrum requires a series of 2D FIDs. It therefore takes longer to acquire, and this is the main reason why 4D spectra are still uncommon. There has recently been development of "reduced dimensionality" methods such as G-matrix Fourier Transform (GFT),[15] which use sums and differences of frequencies to acquire higher dimensional spectra in much reduced time (see Chapters 3 and 6).

Spectral crowding is also reduced, and competing relaxation pathways greatly diminished, by deuteration of some of the protons. Sample preparation is more complex and expensive, but the experiment is identical. With very high levels of deuteration, long mixing times can be used to detect NOEs over distances as large as 12 Å.[16]

18.6 VARIATIONS ON THE NOESY EXPERIMENT

Probably the most useful NOESY variant is the transferred NOE, also known as the exchange-transferred NOE.[3,17,18] This is based on the idea that the buildup of NOEs in a ligand involved in a protein/ligand complex is much faster than in the free ligand. Hence, a NOESY spectrum of a ligand that is in excess over its receptor and in fast exchange will be dominated by NOEs arising from the bound state. The trNOE is therefore very useful for characterizing the structure of a bound ligand, using the much more easily observed and assigned signals for the free ligand. A closely related experiment is cross-saturation, which is used to locate the binding site on protein *B* for protein *A*. Saturation of any resonance in protein *A* leads, by spin diffusion, to saturation of all signals in *A*. When *A* binds to *B*, the saturation will spread to *B* also. This is an elegant experiment, but requires suitable isotopic labeling of both proteins.[19]

A related experiment is saturation transfer difference (STD), and involves saturation of the receptor. Spin diffusion spreads the saturation over the receptor and onto any ligand that is bound to it. Subsequent exchange of the ligand into the free state gives rise to partial saturation of the free ligand, and thus identifies molecules that bind to the receptor. The experiment can be run in 1D or 2D versions.[20]

Heteronuclear NOEs are widely used. Their main application is to measure NOEs on ^{15}N or occasionally ^{13}C from the attached proton: not as a distance measurement but as a way of providing information on molecular motions, because of the sensitivity of cross-relaxation to motion.[3] They are detected by means of HSQC experiments. Observation of specific heteronuclear NOEs has found little application, partly because of its insensitivity, and partly because the heteronuclear NOE is inherently small in almost all the cases where a 2D experiment would be of most applicability, i.e., for large molecules. For example, the maximum NOE to ^{13}C from irradiation of ^{1}H in a slowly tumbling molecule is only 15%. A few applications have appeared, for example, using NOEs involving fluorine, which has a similar gyromagnetic ratio to ^{1}H and therefore gives large NOEs in proteins.[21]

A more complete discussion of recent developments can be found elsewhere.[22]

RELATED ARTICLES IN THE ENCYCLOPEDIA OF MAGNETIC RESONANCE

Biological Macromolecules

Carbohydrates and Glycoconjugates

Composite Pulses

DNA: A-, B-, and Z-

Nuclear Overhauser Effect

Nucleic Acid Structures in Solution: Sequence Dependence

Nucleic Acids: Spectra, Structures, and Dynamics

Phase Cycling

Polysaccharides and Complex Oligosaccharides

Protein Dynamics from NMR Relaxation

Protein Hydration

Protein Structures: Relaxation Matrix Refinement

Relaxation: An Introduction

Relaxation Effects Involving Cross Correlation in Biomolecules

Relaxation Matrix Refinement of Nucleic Acids

Relaxation Processes in Coupled-Spin Systems

Relaxation Processes: Cross Correlation and Interference Terms

Selective NOESY

REFERENCES

1. S. Macura and R. R. Ernst, *Mol. Phys.*, 1980, **41**, 95–117.
2. G. M. Clore and A. M. Gronenborn, *Annu. Rev. Biophys. Biophys. Chem.*, 1991, **20**, 29–63.
3. D. Neuhaus and M. P. Williamson, *The Nuclear Overhauser Effect in Structural and Conformational Analysis*, Wiley-VCH: New York, 2000.
4. H. P. Mo and T. C. Pochapsky, *Prog. NMR Spectrosc.*, 1997, **30**, 1–38.
5. O. W. Sørensen, G. W. Eich, M. H. Levitt, G. Bodenhausen, and R. R. Ernst, *Prog. NMR Spectrosc.*, 1983, **16**, 163–192.
6. P. J. Hore, J. A. Jones, and S. Wimperis, *NMR: The Toolkit*, OUP: Oxford, 2000.
7. A. A. Bothner-By, R. L. Stephens, J. M. Lee, C. D. Warren, and R. W. Jeanloz, *J. Am. Chem. Soc.*, 1984, **106**, 811–813.
8. M. P. Williamson, *Magn. Reson. Chem.*, 1987, **25**, 356–361.
9. M. J. Sutcliffe, in *NMR of Macromolecules*, ed. G. C. K. Roberts, Clarendon Press: Oxford, UK, 1993, Ch. 11.
10. B. A. Borgias, M. Gochin, D. J. Kerwood, and T. L. James, *Prog. NMR Spectrosc.*, 1990, **22**, 83–100.
11. J. Cavanagh, W. J. Fairbrother, A. G. Palmer, and N. J. Skelton, *Protein NMR Spectroscopy*, Academic Press: San Diego, 1996.
12. J. Keeler and D. Neuhaus, *J. Magn. Reson.*, 1985, **63**, 454–472.
13. K. Stott, J. Keeler, Q. N. Van, and A. J. Shaka, *J. Magn. Reson.*, 1997, **125**, 302–324.
14. S. M. Pascal, D. R. Muhandiram, T. Yamazaki, J. D. Forman-Kay, and L. E. Kay, *J. Magn. Reson. B.*, 1994, **103**, 197–201.
15. Y. Shen, H. S. Atreya, G. H. Liu, and T. Szyperski, *J. Am. Chem. Soc.*, 2005, **127**, 9085–9099.
16. R. Sounier, L. Blanchard, Z. R. Wu, and J. Boisbouvier, *J. Am. Chem. Soc.*, 2007, **129**, 472–473.

17. F. Ni, *Prog. NMR Spectrosc.*, 1994, **26**, 517–606.

18. C. B. Post, *Curr. Opin. Struct. Biol.*, 2003, **13**, 581–588.

19. H. Takahashi, T. Nakanishi, K. Kami, Y. Arata, and I. Shimada, *Nat. Struct. Biol.*, 2000, **7**, 220–223.

20. M. Mayer and B. Meyer, *Angew. Chem. Int. Ed. Engl.*, 1999, **38**, 1784–1788.

21. N. J. Baxter, L. F. Olguin, M. Golicnik, G. Feng, A. M. Hounslow, W. Bermel, G. M. Blackburn, F. Hollfelder, J. P. Waltho, and N. H. Williams, *Proc. Natl. Acad. Sci. U.S.A.*, 2006, **103**, 14732–14737.

22. M. P. Williamson, in *Annual Reports on NMR Spectroscopy*, ed. G. A. Webb, Academic Press: London, UK, 2009, Ch. 3.